



UNIVERSITÉ
LAVAL

Experimental Demonstration of a WDM- Compatible Polarization-Diverse OAM Generator and Multiplexer in Silicon Photonics

Yuxuan Chen, Zhongjin Lin, Simon Bélanger-de Villers, Leslie A. Rusch, and Wei Shi

IEEE European Conference on Optical Communications (ECOC 2019)

© 2019 IEEE. Personal use of this material is permitted. Permission from IEEE must be obtained for all other uses, in any current or future media, including reprinting/republishing this material for advertising or promotional purposes, creating new collective works, for resale or redistribution to servers or lists, or reuse of any copyrighted component of this work in other works.

EXPERIMENTAL DEMONSTRATION OF A WDM-COMPATIBLE POLARIZATION-DIVERSE OAM GENERATOR AND MULTIPLEXER IN SILICON PHOTONICS

*Yuxuan Chen, Zhongjin Lin, Simon Bélanger-de Villers, Leslie A. Rusch, Wei Shi**

¹*Department of Electrical and Computer Engineering, Centre for Optics, Photonics and Lasers, Université Laval, Québec, QC, Canada*

**E-mail: wei.shi@gel.ulaval.ca*

Keywords: SILICON PHOTONICS, ORBITAL ANGULAR MOMENTUM, SPACE DIVISION MULTIPLEXING, WAVELENGTH-DIVISION MULTIPLEXING, INTEGRATED PHOTONIC CIRCUITS

Abstract

We design and demonstrate a WDM-compatible polarization-diverse OAM generator and multiplexer. OAM modes with orders from -3 to +3 are generated directly in circular polarization (left or right) within the wavelength range of 1540 nm to 1557 nm.

1 Introduction

Space division multiplexing (SDM) in optical fibre can be combined with multiplexing in time, frequency and polarization, as well as quadrature modulation, to increase the transmission capacity and reduce the cost per bit. Orbital angular momentum (OAM) modes, compared with LP modes, offer a reduction in system complexity and power consumption by avoiding the need for multiple-input, multiple-output pro-cessing [1].

OAM modes can be generated in free-space using spiral phase plates [2], spatial light modulators [3], and q plates [4]. These free-space OAM setups are bulky, hard to align and become quite complex when the number of OAM modes increases. The silicon on insulator (SOI) platform is one of the most promising photonic integration platforms due to its tunability and robustness. Solutions based on silicon resonators [5], [6] has OAM order dependant on the resonance wavelength; these structures are therefore not compatible with wavelength division multiplexing (WDM). In [7], 2D-3D hybrid photonic integrated circuits were used, and the modes generated were either azimuthally or radially polarized, thus, the device cannot directly create the circular polarization required for OAM transmission in fibre [1]. We previously proposed [8] a photonic integrated circuit (PIC) where circularly polarized OAM modes could be directly generated. The PIC was scalable, and we described the design methodology along with transfer-matrix model and optimizing techniques.

In this paper, we design and experimentally demonstrate a WDM-compatible polarization-diverse OAM generator and multiplexer. OAM modes from -3 to +3 order have been generated in both circular polarizations, across the wavelength range of 1540 nm to 1557 nm.

2 Chip design

The schematic of our OAM generator and multiplexer is shown Fig. 1a. The SOI-based circuit is enclosed in the dotted line. The chip optical inputs consist of fibre-to-chip couplers coupled to a single mode fibre (SMF) array. This circuit encodes each input of the SMF array onto a distinct OAM mode and polarization. Each input channel (far left, Fig. 1a) maps to a unique OAM state, distinguished by its polarization, topological charge and direction of rotation of the phase front. The topological charge is an integer, and the direction of rotation is the sign of the topological charge.

The input channels are separated into two sections based on the intended circular polarization state at the output. The input channels that are destined to left circular polarization (LCP) are fed into the left star coupler SC_L , while the input channels destined to right circular polarization (RCP) are fed to right star coupler SC_R . The two star couplers, SC_L and SC_R , perform the exact same task of rotating the phase front based on the intended OAM order implied by the input waveguide position. Assuming only one input port that is destined to LCP is activated, at all the outputs of SC_L , we will see lights with similar amplitude (ideally equal) and uniformly spaced phase.

The difference between SC_L and SC_R is the routing to their outputs. Outputs of SC_L are routed to the upper ports of directional couplers, while outputs of SC_R to the bottom. Above these routing waveguides, we deploy metal for heating on top of each path, allowing us to independently change the refractive index of each waveguide. By heating these elements, we can compensate any phase error during fabrication. The routing waveguides are 65 μm apart to avoid any heat crosstalk from adjacent heaters. Per our design, after the directional coupler, light passing through the directional coupler via the upper port will see a 50-50 splitting ratio and 90-degree phase shift

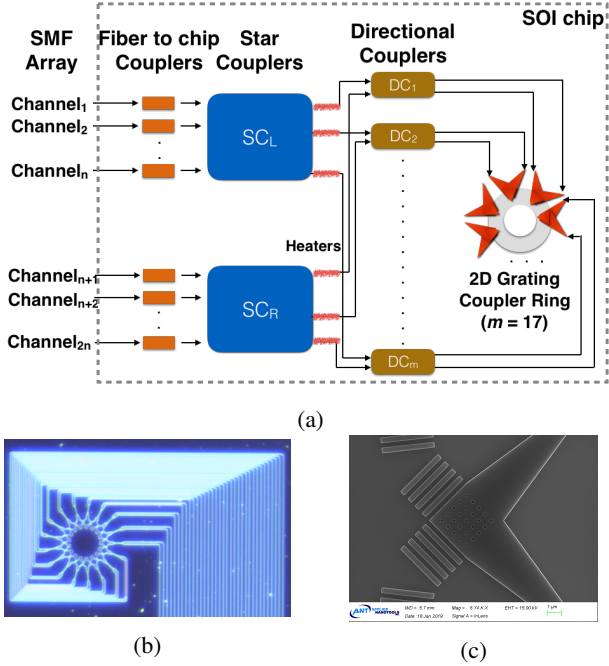


Fig. 1: (a) Schematic of the SOI OAM generator and multiplexer, (b) photograph of fabricated 2D grating coupler ring and directional couplers, and (c) SEM image of one fabricated 2D grating coupler.

between its output ports, while light passing through the bottom port will be evenly split, but with a negative 90-degree phase shift.

The two output ports of each directional coupler are combined by a 2D grating coupler. In this design, 17 of these 2D grating couplers are used in the emitter section. Due to the 90-degree phase difference introduced by the directional coupler, the beam that emits from the 2D grating coupler is circularly polarized. As shown in Fig. 1b, we placed the directional coupler and 2D grating coupler as close as possible to well maintain the 90-degree phase difference and to avoid phase error. In Fig 1c, the scanning electron microscope image of a fabricated 2D grating coupler is shown. We add reflectors after the grating region of the 2D grating coupler to achieve vertical emission for our experimentation.

3 Experimental results

Fig. 2 shows the experimental setup. Our first characterization examines the chip in de-multiplexing mode and focuses on fabrication and using the heaters to correct for phase errors. The second characterization examines the chip in a multiplexing role to confirm generation of the OAM modes (with proper circular polarization) by observing the characteristic spiral interferograms.

The characterization begins by demultiplexing a fundamental mode beam incident on the chip and observing the output ports via the fiber array. The beam from a tunable laser (top right) first passes through a polarization controller for LCP (or RCP) and then strikes the SOI chip. The beam splitter is

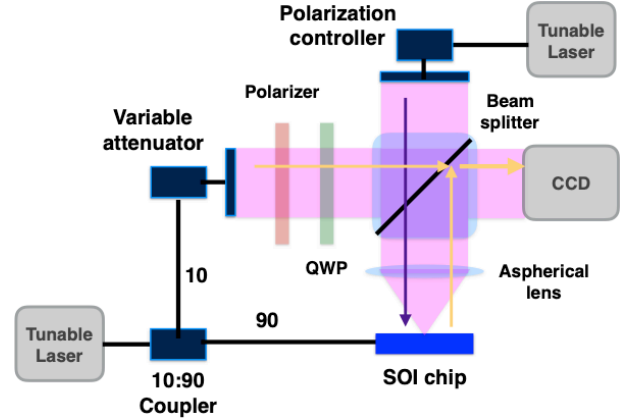


Fig. 2: Experimental setup to characterize chip and observe interference patterns.

assumed to be transparent in this direction. As we set the polarization to left circular, ideally, all the power would go to the output port that corresponds to zeroth order OAM LCP. The power that goes to other ports is crosstalk to other modes.

To compensate for phase errors during fabrication, we sweep the voltage applied on each heating metal from 2V to 6V, until we have maximized the power at the zeroth order port. The same manipulations are done for the RCP branch. After characterization, the highest crosstalk to unwanted modes is -7 dB for LCP and -12 dB for RCP.

To confirm generation of OAM modes, we adjust our setup to generate an interference pattern between the output of the SOI chip and a reference fundamental mode beam. We fix the voltage applied on each heating metal to those optimal values found previously. The top right laser is no longer used.

The beam from the laser on the bottom left is split into two paths at a ratio of 90:10, with 90% of power coupled to the SOI chip through one input of the fiber array. The SOI chip functions as an OAM generator. The beam emitted from the chip is collimated through an aspherical lens and then goes to the beam splitter above it. On the left side of the beam splitter is the reference beam, formed from 10% of the tunable laser. Power of the reference beam is adjusted via a viable attenuator to match the power emitted from the chip. A polarizer and a quarter wave plate are used to produce a circularly polarized reference beam. After the combination of the reference beam and generated beam, interferograms are recorded at the CCD camera to the right.

The input light to the chip is routed to one SOI input at a time, each input corresponding to a target OAM mode and polarization. We interfere the beam generated from the SOI chip with the reference beam twice, once for each circular polarization of the reference beam. The recorded interferograms are shown in Fig. 3. The number on top of each column indicates the intended OAM order (determined by input port). When target and reference polarizations are identical we expect the number of spirals in the interferometer to be equal to the absolute value of the mode order. When the polarizations are

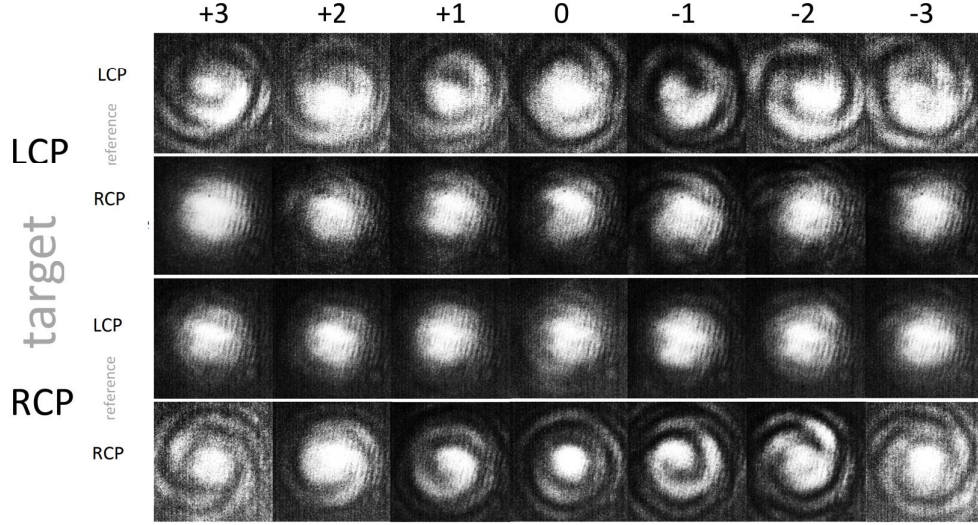


Fig. 3: Interferograms (OAM order appear above columns) for: row 1) LCP generation with LCP reference, row 2) LCP generation with RCP reference, row 3) RCP generation with LCP reference, and row 4) RCP generation with RCP reference.

unaligned, we expect the circular Gaussian intensity pattern in the interferogram.

From Fig. 3, with opposite polarizations between target and reference, we observe Gaussian intensity profiles. For all cases with aligned polarizations we see spiral patterns, confirming generation of OAM beams. The spiral patterns for RCP are in general of greater purity, as expected given the 5 dB difference in crosstalk levels for LCP and RCP observed in the first stage of characterization. The number of spirals observed in each of these interferograms matches with the intended OAM order.

To demonstrate the WDM compatibility of the design, we collected interferograms at four wavelengths for each circular

polarization within the C band. We again fix the voltage applied on each heating metal to those optimal values found previously. Interferogram results are shown in Fig. 4. The maximum and minimum wavelengths indicated the extremes we were able to cover, which are different for LCP and RCP. The overlapping region, 1540 nm to 1557 nm indicates this design, can generate all 7 OAM modes in both circular polarizations (14 information channels) over 17 nm of optical spectrum.

To quantify the wafer non-uniformity, we examined multiple copies of our coupler structure at various locations on the fabricated chip. By comparing six copies of splitting ratio data, the non-uniformity was 2.3 dB for LCP branch and 1.8 dB for RCP (uniform would be 0 dB for each). Starting from the ideal directional coupler model proposed in [8], we introduce this non-uniformity and simulate the resulting interferograms. The deterioration in those interferograms could explain the difference between LCP and RCP branches. A 2×2 multi-mode interference (MMI) coupler could be used to replace the directional coupler for better performance.

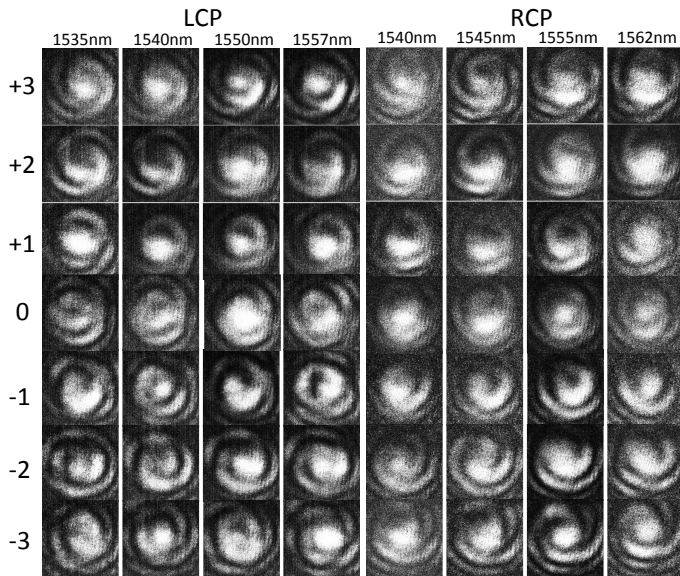


Fig. 4: Interferograms for target and reference beams with identical polarizations for various wavelengths; target OAM orders appear on the left, and polarization and wavelength are indicated above each column.

4 Conclusion

We demonstrated a WDM-compatible polarization-diverse OAM generator and multiplexer that supports up to 3rd order OAM in the fabricated design. Measured interferograms demonstrated OAM spirals of the correct chirality over 17 nm within C band. The design can accommodate more OAM channels by adding 2D grating couplers in the emitter section. As the generated beam is circularly polarized by construction, only minimum free-space optics are needed for OAM fibre coupling.

5 Acknowledgements

This work was supported by Huawei Canada and NSERC (CRDPJ 515539-17).

6 References

- [1] Rusch, L.A., Rad, M., Allahverdyan, K., Fazal, I. and Bernier, E., 2018. Carrying data on the orbital angular momentum of light. *IEEE Communications Magazine*, 56(2), pp.219-224.
- [2] Massari, M., Ruffato, G., Gintoli, M., Ricci, F. and Romanato, F., 2015. Fabrication and characterization of high-quality spiral phase plates for optical applications. *Applied Optics*, 54(13), pp.4077-4083.
- [3] Ohtake, Y., Ando, T., Fukuchi, N., Matsumoto, N., Ito, H. and Hara, T., 2007. Universal generation of higher-order multiringed Laguerre-Gaussian beams by using a spatial light modulator. *Optics letters*, 32(11), pp.1411-1413.
- [4] Karimi, E., Piccirillo, B., Nagali, E., Marrucci, L. and Santamato, E., 2009. Efficient generation and sorting of orbital angular momentum eigenmodes of light by thermally tuned q-plates. *Applied Physics Letters*, 94(23), p.231124.
- [5] Sun, J., Yaacobi, A., Moresco, M., et al., 2014, "Chip-scale continuously tunable optical orbital angular momentum generator", arXiv preprint arXiv:1408.3315.
- [6] Zhang, D., Feng, X. and Huang, Y., "Encoding and decoding of orbital angular momentum for wireless optical interconnects on chip," *Optics Express*, 2012, 20(24), pp. 26986-26995.
- [7] Guan, B., Qin, C., Scott, R.P., et al., October 2015, "Polarization diversified integrated circuits for orbital angular momentum multiplexing," in 2015 IEEE Photonics Conference (IPC), pp. 649-652.
- [8] Chen, Y., Rusch, L.A. and Shi, W., 2018, "Integrated circularly polarized OAM generator and multiplexer for fiber transmission," *IEEE Journal of Quantum Electronics*, 54(2), pp. 1-9.